Discrete Stochastic Arithmetic to Validate the Results of the Nonlinear Fractional Model of Malaria Infection: Application of the CESTAC Method

Samad Noeiaghdam[1,2,*], Aliona Dreglea[2], Hüseyin Isık[3], Muhammad Suleman[4]

[1]South Ural State University, Lenin prospect 76, Chelyabinsk, 454080, Russian Federation.
[2]Baikal School of BRICS, Irkutsk National Research Technical University, Irkutsk, Russian Federation.
[3]Department of Engineering Science, Bandirma Onyedi Eylul University, 10200 Bandirma, Balikesir, Turkey
[4]Department of Mathematics, Comsats University Islamabad, Islamabad 45550, Pakistan.

Abstract

The aim of this paper is to study the nonlinear fractional model of malaria infection based on the Caputo-Fabrizio fractional derivative. After modelizing the phenomenon the Picard-Lindelof approach and the Banach fixed point theorem are applied to show the existence of solution and the stability of the method. For solving the mentioned model, we apply the homotopy analysis transform method (HATM) which is among flexible and accurate methods. For the first time, instead of applying the methods based on the floating-point arithmetic (FPA), we apply the CESTAC method and the CADNA library which are based on the discrete stochastic arithmetic (DSA). This method is one of the main novelties of this study that can help us to validate the obtained results. Using this method, the optimal iteration of the HATM, the optimal approximation and the optimal error can be obtained. Main theorem of the CESTAC method is discussed. Based on this theorem, we will be able to apply a new termination criterion instead of traditional absolute error. By plotting several $\hbar$-curves the convergence regions are demonstrated. Using these graphs we can find the region of convergence for different functions. The numerical results based on the DSA and the FPA are presented in some tables.

keywords: Model of malaria infection, Caputo-Fabrizio derivative, homotopy analysis transform method, CESTAC method, CADNA library.

1 Introduction

Malaria is a life-threatening disease caused by a parasite. The causative agent of this disease to humans is the bite of infected female Anopheles mosquitoes. But malaria is a preventable and treatable disease. According to studies, malaria can be caused by five types of parasites in humans, so that two of them can be a dangerous threat to humans. In 2019, almost half of

*Corresponding author; E-mail: snoei@istu.edu; noiagdams@susu.ru

the world's population was at risk for malaria. Sub-Saharan Africa has the highest mortality rate. In 2019, there were about 229 million malaria cases, and the estimated number of malaria deaths was 409,000 [2].

Given the above, it is easy to understand the importance of examining this disease. Accordingly, various mathematical models have been proposed to control and predict the behavior of this disease according to various human and environmental factors. In [49], the optimal control for a fractional order malaria transmission model was studied, in [15], the comparison of mathematical frameworks for modeling erythropoiesis in the context of malaria infection was illustrated and in [25], the numerical simulation of a reaction-diffusion malaria infection model using B-splines collocation was discussed. The effects of climate change on Plasmodium vivax malaria transmission dynamics based on mathematical models and the endectocide-treated cattle for malaria control are studied in [20, 54].

Solving the mathematical models and finding the accurate and efficient solutions have been investigated by many researchers such as mathematical model of HIV infection [26, 27, 28, 39], model of smoking habit [38], model of computer viruses [29, 30, 45] and many other models [40]. Also, solving fractional models we can find more efficient results than usual models such that recently many researchers have been focused on solving the fractional models based on the Caputo-Fabrizio fractional derivative [26, 28, 40, 48].

The HAM [21, 22, 23] is among semi-analytical and flexible methods for solving various linear and nonlinear problems which by combining the method with Laplace transforms and making the HATM, we can find more accurate results than the traditional HAM. As we know, in this method we are free to choose the auxiliary functions and parameters that it is one of abilities of this method than other methods. The HATM for solving Abel's integral equations of the first kind [46], the homotopy regularization method to solve the singular Volterra integral equations [31], the HAM to solve the first kind Cauchy integral equations arising in the theory of airfoils [10], solving integral equations using the homotopy-regularization method [32] and solving integral equations based on finding the optimal convergence control parameter of the HAM [33] are only some of applications of the HAM and HATM for solving various linear and nonlinear problems.

Generally, the mentioned studies are based on the FPA [11] and researchers apply the absolute error to discuss the accuracy of the methods as follows

$$|f(x) - f_n(x)| < \varepsilon, \tag{1}$$

where $f(x)$ and $f_n(x)$ are exact and approximate solutions of the problem and ε is a small positive value. But this condition can not be acceptable. Why we should solve the problem that we have its exact solution? Also, generally the researchers do not know the optimal value of ε. Also, we can not accept it. If we choose a small value as ε we will have huge number of iterations without improving the accuracy of the results and we will have so many extra iterations. Also, If we choose a large value as ε, the algorithm will be stopped at the first step without producing accurate results. Thus we propose the CESTAC method and the CADNA library which are based on the SA and instead of the stopping condition (1) we have new termination criterion

$$|f_n(x) - f_{n-1}(x)| = @.0, \tag{2}$$

where $f_n(x)$ and $f_{n-1}(x)$ are two successive approximations and @.0 denotes the informatical zero [8, 9, 18]. This sign can be produced only in the CESTAC method by CADNA library and it shows that the number of common significant digits between two successive approximations is almost equal to zero [16, 17, 50, 51]. The CADNA library should be done on Linux operating systems and all CADNA codes should be written using the C, C++, FORTRAN or ADA codes [8]. Recently, many methods have been validated using the CESTAC method and the CADNA library to solve various problems. In [12, 13, 14] the numerical validation of quadrature integration rules were discussed, in [33, 37, 41] the validation of the homotopy analysis method, the Admoian decomposition method and the homotopy perturbation method for solving integral equations were illustrated. [35] is the dynamical validation of Sinc-collocation method for solving fuzzy integral equations, [44] is the dynamical control on load leveling problem and [42] and [34] are the application of the method on the reverse osmosis system. The validation of collocation method for various problems [36, 43] and finding the optimal regularized parameter of the regularization method [32] are some of applications of the CESTAC method and the CADNA library. For more details you can see [11].

2 Preliminaries

In this section, we present some definitions of the fractional derivatives and also the HAM.

2.1 Fractional derivatives

Definition 2.1. *[7] Let g be a continuous function then the ρ-th order Caputo fractional derivative can be defined via integrable differentiations as follows*

$$^{C}\mathfrak{D}^{\rho}g(t) = \frac{1}{\Gamma(n-\rho)}\int_0^t \frac{g^{(n)}(s)}{(t-s)^{\rho-n+1}}ds, \quad n = [\rho]+1.$$

Definition 2.2. *[4] The ρ-th order Caputo-Fabrizio derivative for $b > a, g \in H^1(a,b)$, and $\rho \in (0,1)$ is defined in the following form*

$$^{CF}\mathfrak{D}^{\rho}g(t) = \frac{M(\rho)}{1-\rho}\int_a^t exp\left(\frac{-\rho}{1-\rho}(t-s)\right)g'(s)ds, \quad t \geq 0,$$

where $M(\rho)$ depends on ρ shows a normalization function and $M(0) = M(1) = 1$. For function g which is not member of $H^1(a,b)$, this derivative can be presented for $g \in L^1(-\infty, b)$ as follows:

$$^{CF}\mathfrak{D}^{\rho}g(t) = \frac{\rho M(\rho)}{1-\rho}\int_{-\infty}^b (g(t)-g(s))exp(\frac{-\rho}{1-\rho}(t-s))ds, \quad 0<\rho<1.$$

Also, $\rho+n$-th order fractional derivative $^{CF}\mathfrak{D}^{\rho+n}$ for $n \geq 1$ and $\rho \in (0,1)$ can be defined as $^{CF}\mathfrak{D}^{\rho+n}g(t) :=^{CF} \mathfrak{D}^{\rho}(\mathfrak{D}^n g(t))$.

Definition 2.3. *[24] For $0 < \rho \leq 1$ and $M(\rho) = 1$, the Laplace transform for the Caputo-Fabrizio derivative can be presented in the following form*

$$L[^{CF}\mathfrak{D}^{\rho+n}g(t)](s) = \frac{s^{n+1}L[g(t)] - s^n g(0) - s^{n-1}g'(0) - ... - f^{(n)}(0)}{s + \rho(1-s)}.$$

Definition 2.4. *[24] The ρ-order Riemann-Liouville fractional integral for $Re(\rho) > 0$ is specified as*

$$I^\rho g(t) = \frac{1}{\Gamma(\rho)} \int_0^t (t-s)^{\rho-1} g(s)ds.$$

Definition 2.5. *[24] The fractional integral of Caputo-Fabrizio is defined by*

$$^{CF}I^\rho g(t) = \frac{2(1-\rho)}{(2-\rho)M(\rho)} g(t) + \frac{2(\rho)}{(2-\rho)M(\rho)} \int_0^t g(s)ds, \quad 0 < \rho < 1.$$

Also, the left and right fractional integrals of $(^{CF}_{a}\mathfrak{D}^\rho)$ are defined [3] respectively by

$$(^{CF}I_a^\rho g)(t) = \frac{1-\rho}{B(\rho)} g(t) + \frac{\rho}{B(\rho)} \int_a^t g(s)ds,$$

$$(^{CF}I_b^\rho g)(t) = \frac{1-\rho}{B(\rho)} g(t) + \frac{\rho}{B(\rho)} \int_t^b g(s)ds.$$

e have the following definitions for Sumudu transform which is based on the classical Fourier integral [5, 6, 47].

Definition 2.6. *[6] Let $A = \{G : \exists\lambda, k_1, k_2 \geq 0, |G(t)| < \lambda exp(\frac{t}{k_j}), t \in (-1)^j \times [0, \infty)\}$ then $ST[g(t); u] = G(u)$ shows the Sumudu transform of a function $g(t) \in A$ which is defined as*

$$G(u) = ST[g(t); u] = \frac{1}{u} \int_0^\infty exp(-t/u) g(t)dt, u \in (-k_1, k_2),$$

for all $t \geq 0$. Also, $g(t) = ST^{-1}[G(u)]$ shows the inverse Sumudu transform of $G(u)$.

Definition 2.7. *[5] For $(m–1 < \rho \leq m)$ we can define the Sumudu transform for the Caputo derivative as*

$$ST[^c\mathfrak{D}_t^\rho g(t); u] = u^{-\rho} \left[G(u) - \sum_{i=0}^{m} u^{\rho-i} [^c\mathfrak{D}^{\rho-i} g(t)]_{t=0} \right].$$

Definition 2.8. *[52] Assume that G is a function and it has Caputo–Fabrizio fractional derivative. We can define the Sumudu transform of G with Caputo–Fabrizio fractional derivative as*

$$ST(^{CF}_{0}\mathfrak{D}_t^\rho)(G(t)) = \frac{M(\rho)}{1-\rho+\rho u} [ST(G(t)) - G(0)].$$

Definition 2.9. *[53] For metric space (X, d), a map $g : X \to X$ is called a Picard operator whenever there exists $x^* \in X$ such that $Fix(g) = \{x^*\}$ and the sequence $(g^n(x_0))_{n \in N}$ converges to x^* for all $x_0 \in X$.*

Definition 2.10. *Consider the Banach space* $(Y, \|.\|)$*, a self-map* G *on* Y*, and recursive method* $P_{n+1} = \phi(G, P_n)$*. Let* $\Omega(G)$ *be the fixed point set of* G *which* $\Omega(G) \neq \varnothing$ *and* $\lim_{n\to\infty} P_n = p \in \Omega(G)$*. Suppose that* $\{g_n\} \subset \Omega$ *and* $e_n = g_{n+1} - \phi(G, g_n)$*, if* $\lim_{n\to\infty} e_n = 0$ *implies that* $\lim_{n\to\infty} g_n = p$*, then the recursive procedure* $P_{n+1} = \phi(G, P_n)$ *is* G*-stable. Suppose that our sequence* g_n *has an upper boundary. If Picard's iteration* $P_{n+1} = GP_n$ *is satisfied in all these conditions, then* $P_{n+1} = GP_n$ *is* G*-stable.*

Theorem 2.1. *[53] Assume that* $(Y, \|.\|)$ *is a Banach space and* G *is a self-map of* Y *such that*

$$\|G_x - G_y\| \leq R\|x - G_y\| + r\|x - y\|,$$

for all $x, y \in Y$*, where* $R \geq 0$ *and* $0 \leq r < 1$*. Then* G *is Picard* G*-stable.*

2.2 Homotopy analysis method

Consider the following problem

$$N[u] = 0,$$

where N is a non-linear operator and $u(r)$ is an unknown function. Now, we can define the zero order deformation equation [21, 22, 23] as

$$(1 - v)L\left[U(r; v) - u_0(r)\right] = v\hbar H(r)N\left[U(r; v)\right], \qquad \rho \in [0, 1], \tag{3}$$

where convergence control parameter, linear operator and initial guess denoted by $\hbar, L$ and $u_0(r)$. Also, $H(r) \neq 0$ shows the arbitrary function and $U(r; v)$ is the unknown function which should be determined. We know that $h, H(r)$ are not equal to zero, thus e can write Eq. (3) for $v = 0, 1$ as follows

$$\begin{cases} U(r; 0) = u_0(r), \\ \\ U(r; 1) = u(r). \end{cases} \tag{4}$$

It is obvious that when v increases from 0 to 1, then $U(r; v)$ changes from $u_0(r)$ to $u(r)$ which is called the deformation. Applying the Taylor's theorem we get

$$U(r; v) = u_0(r) + \sum_{m=1}^{\infty} u_m(r)v^m, \tag{5}$$

where

$$u_m(r) = \frac{1}{m!}\frac{\partial^m U(r; v)}{\partial v^m} \mid_{v=0} .$$

If we find comfortable values and functions for $L, \hbar, H(r)$ and $u_0(r)$, then the series (5) will be convergent at $v = 1$. Now, we can write the series solution in the following form

$$u_m(r) = U(r; 1) = u_0(r) + \sum_{m=1}^{\infty} u_m(r).$$

In order to construct the m-th order deformation equation, the following vector is defined

$$\overrightarrow{u}_j(r) = \{u_0(r), u_1(r), ..., u_j(r)\},$$

By m-times differentiating the Eq. (3) relative to v and then dividing to $m!$ and putting $v = 0$, we can find the m-th order deformation equation as

$$L\big[u_m(r) - \chi_m u_{m-1}(r)\big] = \hbar H(r)\Re_m\big(u_{m-1}^{\rightarrow}(r)\big), \tag{6}$$

where

$$\Re_m(u_{m-1}^{\rightarrow}(r)) = \frac{1}{(m-1)!}\frac{\partial^{m-1}N[U(r;v)]}{\partial v^{m-1}}\bigg|_{v=0}, \tag{7}$$

and

$$\chi_m = \begin{cases} 0, & m \leqslant 1, \\ \\ 1, & m > 1. \end{cases}$$

The j-th order approximate solution can be obtained by $U_j(r) = \sum_{m=0}^{j} u_m(r)$ and for the exact solution we have

$$U(r) = \lim_{j\to\infty} u_j(r).$$

3 Mathematical model of Malaria infection

The aim of this paper is to present the HATM to solve the following non-linear bio-mathematical model

$$\begin{cases} \dfrac{dI}{dt} = mP_H\beta_H SZ - (\varepsilon + \mu_H)I, \\ \\ \dfrac{dR}{dt} = \varepsilon I + kA - (\theta m P_H\beta_H Z + \tau + \mu_H)R, \\ \\ \dfrac{dA}{dt} = \theta m P_H\beta_H RZ - (k + \mu_H)A, \\ \\ \dfrac{dY}{dt} = P_H\beta_Z(I + \sigma A)X - (\xi + \mu_v)Y, \\ \\ \dfrac{dZ}{dt} = \xi Y - \mu_v Z. \end{cases} \tag{8}$$

an infectious mosquito 'Z', will bite 'S'usceptible hosts and make them 'I'nfected. We know that infected hosts before reversion to fully susceptible at rate $'\tau'$ can have level of temporary immunity ($1 - \theta$, where $0 \leq \theta \leq 1$). However, we should note that hosts can become 'A'symptomatically infected during this 'R'ecovered state. Symptomatic infection is a temporary condition that may have different transmission potentials to (*sigma*) carriers, after which people return to the improved group at a rate of *kappa*. In this model, considering that a fixed human population is assumed, human mortality is compensated by births and we get $S = 1-(I+R+A)$. Sensitive (X) vectors begin to become infected after being bitten by an infected infectious host, but they are not yet infected (Y), but after the extrinsic incubation period $(\frac{1}{\xi})$, become infectious (Z). We apply m to show the ratio of vector-to-hosts which vectors typically outnumber hosts. Here, a stable vector population is assumed whereby births are set to balance deaths (μ_v) and so $X = 1-(Y+Z)$. Parameter values and literature sources are detailed in Table 1.

Table 1: List of parameters and functions [54].

Parameters	Meaning	Values
β_z	Transmission coefficient (vectors $\to$ hosts) = bite rate $\times$ transmission probability	$0.1 = \frac{1}{3} \times 0.3$
β_H	Transmission coefficient (hosts $\to$ vectors) = bite rate $\times$ transmission probability	$0.007 = \frac{1}{3} \times 0.02$
ε	Clearance rate of symptomatic infection	$\frac{1}{200}$
μ_H	Birth and death rate of humans (i.e., stable population)	$\frac{1}{21900}$
k	Clearance rate of asymptomatic infection	$\frac{1}{200}$
θ	Asymptomatic secondary infection rate	0.5
τ	Full susceptibility reversion rate	$\frac{1}{1000}$
σ	Adjustment factor for asymptomatic transmissibility to vector	0.25
μ_v	Birth (or maturation) and death rate of vectors (i.e., stable population)	0.1
ξ	Rate of parasite development within vector	0.1

Applying the ρ-th order Caputo–Fabrizio fractional derivative instead of the first order time derivative we have

$$\begin{cases} {}_0^{CF}\mathfrak{D}_t^{\rho} I = mP_H\beta_H SZ - (\varepsilon+\mu_H)I, \\ {}_0^{CF}\mathfrak{D}_t^{\rho} R = \varepsilon I + kA - (\theta m P_H\beta_H Z + \tau + \mu_H)R, \\ {}_0^{CF}\mathfrak{D}_t^{\rho} A = \theta m P_H \beta_H RZ - (k+\mu_H)A, \\ {}_0^{CF}\mathfrak{D}_t^{\rho} Y = P_H\beta_Z(I+\sigma A)X - (\xi+\mu_v)Y, \\ {}_0^{CF}\mathfrak{D}_t^{\rho} Z = \xi Y - \mu_v Z, \end{cases} \tag{9}$$

where $0<\rho\le 1$ and $I(0)=I_0, R(0)=R_0, A(0)=A_0, Y(0)=Y_0$ and $Z(0)=Z_0$.

4 Existence of solution

Consider the mathematical model (9) which applying the Losada and Nieto integral operator [24] we get

$$
\left\{
\begin{aligned}
I(t) - g_1(t) &= \frac{2(1-\rho)}{(2-\rho)M(\rho)}\{mP_H\beta_H S(t)Z(t) - (\varepsilon + \mu_H)I(t)\} \\
&\quad + \frac{2\rho}{(2-\rho)M(\rho)}\int_0^t [mP_H\beta_H S(s)Z(s) - (\varepsilon + \mu_H)I(s)]ds, \\
R(t) - g_2(t) &= \frac{2(1-\rho)}{(2-\rho)M(\rho)}\{\varepsilon I(t) + kA(t) - (\theta m P_H\beta_H Z(t) + \tau + \mu_H)R(t)\} \\
&\quad + \frac{2\rho}{(2-\rho)M(\rho)}\int_0^t [\varepsilon I(s) + kA(s) - (\theta m P_H\beta_H Z(s) + \tau + \mu_H)R(s)]ds, \\
A(t) - g_3(t) &= \frac{2(1-\rho)}{(2-\rho)M(\rho)}\{\theta m P_H\beta_H R(t)Z(t) - (k + \mu_H)A(t)\} \\
&\quad + \frac{2\rho}{(2-\rho)M(\rho)}\int_0^t [\theta m P_H\beta_H R(s)Z(s) - (k + \mu_H)A(s)]ds, \\
Y(t) - g_4(t) &= \frac{2(1-\rho)}{(2-\rho)M(\rho)}\{P_H\beta_Z(I(t) + \sigma A(t))X(t) - (\xi + \mu_v)Y(t)\} \\
&\quad + \frac{2\rho}{(2-\rho)M(\rho)}\int_0^t [P_H\beta_Z(I(s) + \sigma A(s))X(s) - (\xi + \mu_v)Y(s)]ds, \\
Z(t) - g_5(t) &= \frac{2(1-\rho)}{(2-\rho)M(\rho)}\{\xi Y(t) - \mu_v Z(t)\} \\
&\quad + \frac{2\rho}{(2-\rho)M(\rho)}\int_0^t [\xi Y(s) - \mu_v Z(s)]ds.
\end{aligned}
\right. \tag{10}
$$

By assuming $I_0(t) = g_1(t), R_0(t) = g_2(t), A_0(t) = g_3(t), Y_0(t) = g_4(t)$ and $Z_0(t) = g_5(t)$, Eq.

(10) can be written as follows

$$
\begin{cases}
I_{n+1}(t) &= \dfrac{2(1-\rho)}{(2-\rho)M(\rho)}\{mP_H\beta_H S_n(t)Z_n(t) - (\varepsilon+\mu_H)I_n(t)\} \\
&+ \dfrac{2\rho}{(2-\rho)M(\rho)}\displaystyle\int_0^t [mP_H\beta_H S_n(s)Z_n(s) - (\varepsilon+\mu_H)I_n(s)]ds, \\
R_{n+1}(t) &= \dfrac{2(1-\rho)}{(2-\rho)M(\rho)}\{\varepsilon I_n(t) + kA_n(t) - (\theta mP_H\beta_H Z_n(t) + \tau + \mu_H)R_n(t)\} \\
&+ \dfrac{2\rho}{(2-\rho)M(\rho)}\displaystyle\int_0^t [\varepsilon I_n(s) + kA_n(s) - (\theta mP_H\beta_H Z_n(s) + \tau + \mu_H)R_n(s)]ds, \\
A_{n+1}(t) &= \dfrac{2(1-\rho)}{(2-\rho)M(\rho)}\{\theta mP_H\beta_H R_n(t)Z_n(t) - (k+\mu_H)A_n(t)\} \\
&+ \dfrac{2\rho}{(2-\rho)M(\rho)}\displaystyle\int_0^t [\theta mP_H\beta_H R_n(s)Z_n(s) - (k+\mu_H)A_n(s)]ds, \\
Y_{n+1}(t) &= \dfrac{2(1-\rho)}{(2-\rho)M(\rho)}\{P_H\beta_Z(I_n(t) + \sigma A_n(t))X_n(t) - (\xi+\mu_v)Y_n(t)\} \\
&+ \dfrac{2\rho}{(2-\rho)M(\rho)}\displaystyle\int_0^t [P_H\beta_Z(I_n(s) + \sigma A_n(s))X_n(s) - (\xi+\mu_v)Y_n(s)]ds, \\
Z_{n+1}(t) &= \dfrac{2(1-\rho)}{(2-\rho)M(\rho)}\{\xi Y_n(t) - \mu_v Z_n(t)\} \\
&+ \dfrac{2\rho}{(2-\rho)M(\rho)}\displaystyle\int_0^t [\xi Y_n(s) - \mu_v Z_n(s)]ds.
\end{cases} \tag{11}
$$

Applying limitation for series (11) when n approaches infinity, the exact solutions can be obtained as

$$
\begin{aligned}
&\lim_{n\to\infty} I_n(t) = I(t), \\
&\lim_{n\to\infty} R_n(t) = R(t), \\
&\lim_{n\to\infty} A_n(t) = A(t), \\
&\lim_{n\to\infty} Y_n(t) = Y(t), \\
&\lim_{n\to\infty} Z_n(t) = Z(t).
\end{aligned} \tag{12}
$$

4.1 Existence of solution by the Picard-Lindelof approach

In order to prove the existence theorem, the Picard–Lindelof approach and the Banach fixed point theorem are applied. For this aim, the following operators are defined

$$\begin{cases} g_1(t, I) = mP_H\beta_H SZ - (\varepsilon + \mu_H)I, \\ g_2(t, R) = \varepsilon I + kA - (\theta mP_H\beta_H Z + \tau + \mu_H)R, \\ g_3(t, A) = \theta mP_H\beta_H RZ - (k + \mu_H)A, \\ g_4(t, Y) = P_H\beta_Z(I + \sigma A)X - (\xi + \mu_v)Y, \\ g_5(t, Z) = \xi Y - \mu_v Z. \end{cases} \tag{13}$$

Assume that

$$\begin{aligned} L_1 &= \sup_{C[a,c_1]} \|g_1(t, I)\|, \\ L_2 &= \sup_{C[a,c_2]} \|g_1(t, R)\|, \\ L_3 &= \sup_{C[a,c_3]} \|g_1(t, A)\|, \\ L_4 &= \sup_{C[a,c_c]} \|g_1(t, Y)\|, \\ L_5 &= \sup_{C[a,c_c]} \|g_1(t, Z)\|, \end{aligned} \tag{14}$$

where

$$\begin{cases} C[a, c_1] = |t - a, t + a| \times |I - c_1, I + c_1| = A \times C_1, \\ C[a, c_2] = |t - a, t + a| \times |R - c_2, R + c_2| = A \times C_2, \\ C[a, c_3] = |t - a, t + a| \times |A - c_3, A + c_3| = A \times C_3, \\ C[a, c_4] = |t - a, t + a| \times |Y - c_4, Y + c_4| = A \times C_4, \\ C[a, c_5] = |t - a, t + a| \times |Z - c_5, Z + c_5| = A \times C_5. \end{cases} \tag{15}$$

Let

$$\|Y(t)\|_\infty = \sup_{t \in [t-a,t+a]} |Y(t)|, \tag{16}$$

be a uniform norm on $C[a, c_i], i = 1, ..., 5$.

Consider the following Picard operator

$$O : C(A, C_1, C_2, C_3, C_4, C_5) \to C(A, C_1, C_2, C_3, C_4, C_5), \tag{17}$$

which is presented as

$$O(Y(t)) = Y_0(t) + \frac{2(1-\rho)}{(2-\rho)M(\rho)} G(t, Y(t)) + \frac{2\rho}{(2-\rho)M(\rho)} \int_0^t G(s, Y(s))ds, \tag{18}$$

where $Y(t) = \{I(t), R(t), A(t), Y(t), Z(t)\}$ and $Y_0(t) = \{I(0), R(0), A(0), Y(0), Z(0)\}$ and

$$G(t, Y(t)) = \{g_1(t, I), g_2(t, R), g_3(t, A), g_4(t, Y), g_5(t, Z)\}. \tag{19}$$

By assuming that the solutions of the problem are bounded within a time period we can write

$$\|Y(t)\|_\infty \leq \max\{c_1, ..., c_5\} = C. \tag{20}$$

For $L = \max\{L_1, ..., L_5\}$ there is t_0 such that $t_0 \geq t$, then we get

$$\begin{aligned}
\|O(Y(t)) - Y_0(t)\| &= \|\frac{2(1-\rho)}{(2-\rho)M(\rho)} G(t, Y(t)) + \frac{2\rho}{(2-\rho)M(\rho)} \int_0^t G(s, Y(s))ds\| \\
&\leq \frac{2(1-\rho)}{(2-\rho)M(\rho)} \|G(t, Y(t))\| + \frac{2\rho}{(2-\rho)M(\rho)} \int_0^t \|G(s, Y(s))\|ds \qquad (21) \\
&\leq \left(\frac{2(1-\rho)}{(2-\rho)M(\rho)} + \frac{2\rho t}{(2-\rho)M(\rho)}\right) L \\
&\quad \leq \left(\frac{2(1-\rho)}{(2-\rho)M(\rho)} + \frac{2\rho t_0}{(2-\rho)M(\rho)}\right) L \leq \mu L \leq C, \qquad (22)
\end{aligned}$$

where

$$\mu < \frac{C}{L}. \tag{23}$$

Also, we get

$$\|OY_1 - OY_2\| = \sup_{t \in A} |Y_1(t) - Y_2(t)|. \tag{24}$$

Applying the definition of our Picard operator, the following operator can be obtained

$$
\begin{aligned}
\|OY_1 - OY_2\| &= \|\frac{2(1-\rho)}{(2-\rho)M(\rho)}\{G(t, Y_1(t)) - G(t, Y_2(t))\} \\
&+\frac{2\rho}{(2-\rho)M(\rho)}\int_0^t \{G(s, Y_1(s)) - G(s, Y_2(s))\}ds\| \\
&\leq \frac{2(1-\rho)}{(2-\rho)M(\rho)}\|G(t, Y_1(t)) - G(t, Y_2(t))\| \\
&+\frac{2\rho}{(2-\rho)M(\rho)}\int_0^t \|G(s, Y_1(s)) - G(s, Y_2(s))\|ds \\
&\leq \frac{2(1-\rho)}{(2-\rho)M(\rho)}\lambda\|Y_1(t) - Y_2(t)\| \\
&+\frac{2\rho\lambda}{(2-\rho)M(\rho)}\int_0^t \|Y_1(s) - Y_2(s)\|ds \\
&\leq \left(\frac{2(1-\rho)\lambda}{(2-\rho)M(\rho)} + \frac{2\rho\lambda t_0}{(2-\rho)M(\rho)}\right)\|Y_1(t) - Y_2(t)\| \\
&\leq \mu\lambda\|Y_1(t) - Y_2(t)\|
\end{aligned} \tag{25}
$$

where $\lambda < 1$. We know that G is a contraction so $\mu\lambda < 1$ and O is a contraction and it shows that the proof is complete.

5 Special solution via iteration approach

In this section, we can present a special solution of (9). Using the Sumudu transformation for both sided of (9) we get

$$
\begin{cases}
ST({}_0^{CF}\mathfrak{D}_t^\rho I(t)) = ST(mP_H\beta_H S(t)Z(t) - (\varepsilon + \mu_H)I(t)), \\
ST({}_0^{CF}\mathfrak{D}_t^\rho R(t)) = ST(\varepsilon I(t) + kA(t) - (\theta mP_H\beta_H Z(t) + \tau + \mu_H)R(t)), \\
ST({}_0^{CF}\mathfrak{D}_t^\rho A(t)) = ST(\theta mP_H\beta_H R(t)Z(t) - (k + \mu_H)A(t)), \\
ST({}_0^{CF}\mathfrak{D}_t^\rho Y(t)) = ST(P_H\beta_Z(I(t) + \sigma A(t))X - (\xi + \mu_v)Y(t)), \\
ST({}_0^{CF}\mathfrak{D}_t^\rho Z(t)) = ST(\xi Y(t) - \mu_v Z(t)).
\end{cases} \tag{26}
$$

Then we can write

$$
\begin{cases}
\frac{M(\rho)}{1-\rho+\rho u}(ST(I(t))-I(0)) = ST(mP_H\beta_H S(t)Z(t)-(\varepsilon+\mu_H)I(t)), \\
\frac{M(\rho)}{1-\rho+\rho u}(ST(R(t))-R(0)) = ST(\varepsilon I(t)+kA(t)-(\theta mP_H\beta_H Z(t)+\tau+\mu_H)R(t)), \\
\frac{M(\rho)}{1-\rho+\rho u}(ST(A(t))-A(0)) = ST(\theta mP_H\beta_H R(t)Z(t)-(k+\mu_H)A(t)), \\
\frac{M(\rho)}{1-\rho+\rho u}(ST(Y(t))-Y(0)) = ST(P_H\beta_Z(I(t)+\sigma A(t))X-(\xi+\mu_v)Y(t)), \\
\frac{M(\rho)}{1-\rho+\rho u}(ST(Z(t))-Z(0)) = ST(\xi Y(t)-\mu_v Z(t)),
\end{cases} \tag{27}
$$

and we get

$$
\begin{cases}
ST(I(t)) = I(0)+\frac{1-\rho+\rho u}{M(\rho)}ST(mP_H\beta_H S(t)Z(t)-(\varepsilon+\mu_H)I(t)), \\
ST(R(t)) = R(0)+\frac{1-\rho+\rho u}{M(\rho)}ST(\varepsilon I(t)+kA(t)-(\theta mP_H\beta_H Z(t)+\tau+\mu_H)R(t)), \\
ST(A(t)) = A(0)+\frac{1-\rho+\rho u}{M(\rho)}ST(\theta mP_H\beta_H R(t)Z(t)-(k+\mu_H)A(t)), \\
ST(Y(t)) = Y(0)+\frac{1-\rho+\rho u}{M(\rho)}ST(P_H\beta_Z(I(t)+\sigma A(t))X-(\xi+\mu_v)Y(t)), \\
ST(Z(t)) = Z(0)+\frac{1-\rho+\rho u}{M(\rho)}ST(\xi Y(t)-\mu_v Z(t)).
\end{cases} \tag{28}
$$

Finally, the following iterative relation is received

$$\begin{cases} I_{n+1}(t) = I_n(t) + ST^{-1}\left\{\dfrac{1-\rho+\rho u}{M(\rho)} ST(mP_H\beta_H S_n(t)Z_n(t) - (\varepsilon+\mu_H)I_n(t))\right\}, \\ R_{n+1}(t) = R_n(t) + ST^{-1}\left\{\dfrac{1-\rho+\rho u}{M(\rho)} ST(\varepsilon I_n(t) + kA_n(t) - (\theta m P_H\beta_H Z_n(t) + \tau + \mu_H)R_n(t))\right\}, \\ A_{n+1}(t) = A_n(t) + ST^{-1}\left\{\dfrac{1-\rho+\rho u}{M(\rho)} ST(\theta m P_H\beta_H R_n(t)Z_n(t) - (k+\mu_H)A_n(t))\right\}, \\ Y_{n+1}(t) = Y_n(t) + ST^{-1}\left\{\dfrac{1-\rho+\rho u}{M(\rho)} ST(P_H\beta_Z(I_n(t)+\sigma A_n(t))X - (\xi+\mu_v)Y_n(t))\right\}, \\ Z_{n+1}(t) = Z_n(t) + ST^{-1}\left\{\dfrac{1-\rho+\rho u}{M(\rho)} ST(\xi Y_n(t) - \mu_v Z_n(t))\right\}, \end{cases} \tag{29}$$

and the solution can be obtained using

$$\begin{aligned} &\lim_{n\to\infty} I_n(t) = I(t), \\ &\lim_{n\to\infty} R_n(t) = R(t), \\ &\lim_{n\to\infty} A_n(t) = A(t), \\ &\lim_{n\to\infty} Y_n(t) = Y(t), \\ &\lim_{n\to\infty} Z_n(t) = Z(t). \end{aligned} \tag{30}$$

5.1 Fixed point theorem for stability analysis of the iteration method

Theorem 5.1. *Assume that F is a self-map which is defined as follows*

$$\begin{cases} F(I_n(t)) = I_{n+1}(t) = I_n(t) + ST^{-1}\left\{\dfrac{1-\rho+\rho u}{M(\rho)} ST(mP_H\beta_H S_n(t)Z_n(t) - (\varepsilon+\mu_H)I_n(t))\right\}, \\ F(R_n(t)) = R_{n+1}(t) = R_n(t) + ST^{-1}\Big\{\dfrac{1-\rho+\rho u}{M(\rho)} ST(\varepsilon I_n(t) + kA_n(t) \\ \qquad\qquad - (\theta m P_H\beta_H Z_n(t) + \tau + \mu_H)R_n(t))\Big\}, \\ F(A_n(t)) = A_{n+1}(t) = A_n(t) + ST^{-1}\left\{\dfrac{1-\rho+\rho u}{M(\rho)} ST(\theta m P_H\beta_H R_n(t)Z_n(t) - (k+\mu_H)A_n(t))\right\}, \\ F(Y_n(t)) = Y_{n+1}(t) = Y_n(t) + ST^{-1}\left\{\dfrac{1-\rho+\rho u}{M(\rho)} ST(P_H\beta_Z(I_n(t)+\sigma A_n(t))X - (\xi+\mu_v)Y_n(t))\right\}, \\ F(Z_n(t)) = Z_{n+1}(t) = Z_n(t) + ST^{-1}\left\{\dfrac{1-\rho+\rho u}{M(\rho)} ST(\xi Y_n(t) - \mu_v Z_n(t))\right\}, \end{cases} \tag{31}$$

then (31) is F-stable in $L^1(a,b)$ if

$$\begin{cases} \{1 + mP_H\beta_H M_6 f_1(\eta) + mP_H\beta_H M_5 f_2(\eta) - (\varepsilon+\mu_H)M_6 f_3(\eta)\} < 1, \\ \{1 + \varepsilon f_4(\eta) + k f_5(\eta) - \theta m P_H\beta_H M_5 f_6(\eta) - \theta m P_H\beta_H M_2 f_7(\eta) + (\tau+\mu_H) f_8(\eta)\} < 1, \\ \{1 + \theta m P_H\beta_H M_2 f_9(\eta) + \theta m P_H\beta_H M_5 f_{10}(\eta) - (k+\mu_H) f_{11}(\eta)\} < 1, \\ \{1 + P_H\beta_Z M_1 f_{12}(\eta) + P_H\beta_Z M_7 f_{13}(\eta) + \sigma M_3 f_{14}(\eta) + \sigma M_7 f_{15}(\eta) - (\xi+\mu_v) f_{16}(\eta)\} < 1, \\ \{1 + \xi f_{17}(\eta) - \mu_v f_{18}(\eta)\} < 1. \end{cases} \tag{32}$$

Proof: We should show that for $(n,m) \in N \times N$, F has a fixed point:

$$\begin{cases} F(I_n(t)) - F(I_m(t)) \\ = I_n - I_m + ST^{-1}\left\{\frac{1-\rho+\rho u}{M(\rho)} ST(mP_H\beta_H S_n(t)Z_n(t) - (\varepsilon+\mu_H)I_n(t))\right\} \\ -ST^{-1}\left\{\frac{1-\rho+\rho u}{M(\rho)} ST(mP_H\beta_H S_m(t)Z_m(t) - (\varepsilon+\mu_H)I_m(t))\right\}. \end{cases} \tag{33}$$

Using norm for Eq. (33) we have

$$\begin{cases} \|F(I_n) - F(I_m)\| \\ = \|I_n - I_m + ST^{-1}\left\{\frac{1-\rho+\rho u}{M(\rho)} ST(mP_H\beta_H(S_nZ_n - S_mZ_m) - (\varepsilon+\mu_H)(I_n - I_m))\right\}\| \\ \leq \|I_n - I_m\| + ST^{-1}\Big\{\frac{1-\rho+\rho u}{M(\rho)} ST(\|mP_H\beta_H S_n(Z_n - Z_m)\| + \|mP_H\beta_H Z_m(S_n - S_m)\| \\ \qquad\qquad + \| - (\varepsilon+\mu_H)(I_n - I_m)\|)\Big\}. \end{cases} \tag{34}$$

Because of the same role of both solutions, we get

$$\begin{cases} \|I_n(t) - I_m(t)\| \cong \|R_n(t) - R_m(t)\| \cong \|A_n(t) - A_m(t)\| \\ \|Y_n(t) - Y_m(t)\| \cong \|Z_n(t) - Z_m(t)\|. \end{cases} \tag{35}$$

Using relations (34) and (35) we can write

$$\begin{cases} \|F(I_n(t)) - F(I_m(t))\| \\ \leq \|I_n(t) - I_m(t)\| + ST^{-1}\Big\{\frac{1-\rho+\rho u}{M(\rho)} ST(\|mP_H\beta_H S_n(t)(I_n(t) - I_m(t))\| \\ \qquad\qquad + \|mP_H\beta_H Z_m(t)(I_n(t) - I_m(t))\| + \| - (\varepsilon+\mu_H)(I_n - I_m)\|)\Big\}. \end{cases} \tag{36}$$

We know that I_n, R_n, A_n, Y_n, Z_n are bounded because they are convergent sequences, thus there are M_1, M_2, M_3, M_4, M_5 for all t such that

$$\|I_n\| < M_1, \|R_n\| < M_2, \|A_n\| < M_3, \|Y_n\| < M_4, \|Z_n\| < M_5, \|S_n\| < M_6, \|X_n\| < M_7, \tag{37}$$

where $(m, n) \in N \times N$. Applying Eqs. (36) and (37) we can write

$$\begin{cases} \|F(I_n(t)) - F(I_m(t))\| \\ \leq \{1 + mP_H\beta_H M_6 f_1(\eta) + mP_H\beta_H M_5 f_2(\eta) - (\varepsilon+\mu_H)M_6 f_3(\eta)\} \|I_n(t) - I_m(t)\| \end{cases} \tag{38}$$

where f_i are functions from $ST^{-1}\left\{\frac{1-\rho+\rho u}{M(\rho)} ST\left(.\right)\right\}$. By repeating the process we get

$$\begin{cases} \|F(R_n(t)) - F(R_m(t))\| \leq \Big\{1 + \varepsilon f_4(\eta) + k f_5(\eta) - \theta m P_H \beta_H M_5 f_6(\eta) - \theta m P_H \beta_H M_2 f_7(\eta) \\ \qquad\qquad + (\tau + \mu_H) f_8(\eta)\Big\} \|R_n(t) - R_m(t)\|, \\ \|F(A_n(t)) - F(A_m(t))\| \leq \Big\{1 + \theta m P_H \beta_H M_2 f_9(\eta) + \theta m P_H \beta_H M_5 f_{10}(\eta) \\ \qquad\qquad - (k + \mu_H) f_{11}(\eta)\Big\} \|A_n(t) - A_m(t)\|, \\ \|F(Y_n(t)) - F(Y_m(t))\| \leq \Big\{1 + P_H \beta_Z M_1 f_{12}(\eta) + P_H \beta_Z M_7 f_{13}(\eta) + \sigma M_3 f_{14}(\eta) \\ \qquad\qquad + \sigma M_7 f_{15}(\eta) - (\xi + \mu_v) f_{16}(\eta)\Big\} \|Y_n(t) - Y_m(t)\|, \\ \|F(Z_n(t)) - F(Z_m(t))\| \leq \{1 + \xi f_{17}(\eta) - \mu_v f_{18}(\eta)\} \|Z_n(t) - Z_m(t)\|. \end{cases} \tag{39}$$

where

$$\begin{cases} \{1 + m P_H \beta_H M_6 f_1(\eta) + m P_H \beta_H M_5 f_2(\eta) - (\varepsilon + \mu_H) M_6 f_3(\eta)\} < 1, \\ \{1 + \varepsilon f_4(\eta) + k f_5(\eta) - \theta m P_H \beta_H M_5 f_6(\eta) - \theta m P_H \beta_H M_2 f_7(\eta) + (\tau + \mu_H) f_8(\eta)\} < 1, \\ \{1 + \theta m P_H \beta_H M_2 f_9(\eta) + \theta m P_H \beta_H M_5 f_{10}(\eta) - (k + \mu_H) f_{11}(\eta)\} < 1, \\ \{1 + P_H \beta_Z M_1 f_{12}(\eta) + P_H \beta_Z M_7 f_{13}(\eta) + \sigma M_3 f_{14}(\eta) + \sigma M_7 f_{15}(\eta) - (\xi + \mu_v) f_{16}(\eta)\} < 1, \\ \{1 + \xi f_{17}(\eta) - \mu_v f_{18}(\eta)\} < 1. \end{cases} \tag{40}$$

Then the F self-mapping has a fixed point. In addition, we show that F satisfies the conditions in Theorem 2.1. Suppose that (38) and (39) hold, then we get $R = (0, 0, 0, 0, 0)$ and

$$r = \begin{cases} \{1 + m P_H \beta_H M_6 f_1(\eta) + m P_H \beta_H M_5 f_2(\eta) - (\varepsilon + \mu_H) M_6 f_3(\eta)\}, \\ \{1 + \varepsilon f_4(\eta) + k f_5(\eta) - \theta m P_H \beta_H M_5 f_6(\eta) - \theta m P_H \beta_H M_2 f_7(\eta) + (\tau + \mu_H) f_8(\eta)\}, \\ \{1 + \theta m P_H \beta_H M_2 f_9(\eta) + \theta m P_H \beta_H M_5 f_{10}(\eta) - (k + \mu_H) f_{11}(\eta)\}, \\ \{1 + P_H \beta_Z M_1 f_{12}(\eta) + P_H \beta_Z M_7 f_{13}(\eta) + \sigma M_3 f_{14}(\eta) + \sigma M_7 f_{15}(\eta) - (\xi + \mu_v) f_{16}(\eta)\}, \\ \{1 + \xi f_{17}(\eta) - \mu_v f_{18}(\eta)\}, \end{cases} \tag{41}$$

and it shows that all conditions of Theorem 2.1 are satisfied. Thus proof is complete.

6 Application of the HATM to solve the model

Applying the Laplace transform for both sides of Eq. (9) we get

$$\begin{cases} L[{}_{0}^{CF}\mathfrak{D}_{t}^{\rho}I] = L[mP_{H}\beta_{H}SZ - (\varepsilon+\mu_{H})I], \\ L[{}_{0}^{CF}\mathfrak{D}_{t}^{\rho}R] = L[\varepsilon I + kA - (\theta mP_{H}\beta_{H}Z + \tau + \mu_{H})R], \\ L[{}_{0}^{CF}\mathfrak{D}_{t}^{\rho}A] = L[\theta mP_{H}\beta_{H}RZ - (k+\mu_{H})A], \\ L[{}_{0}^{CF}\mathfrak{D}_{t}^{\rho}Y] = L[P_{H}\beta_{Z}(I+\sigma A)X - (\xi+\mu_{v})Y], \\ L[{}_{0}^{CF}\mathfrak{D}_{t}^{\rho}Z] = L[\xi Y - \mu_{v}Z], \end{cases} \tag{42}$$

and we can write

$$\begin{cases} \dfrac{sL(I)-I(0)}{s+\rho(1-s)} = L[mP_{H}\beta_{H}SZ - (\varepsilon+\mu_{H})I], \\ \dfrac{sL(R)-R(0)}{s+\rho(1-s)} = L[\varepsilon I + kA - (\theta mP_{H}\beta_{H}Z + \tau + \mu_{H})R], \\ \dfrac{sL(A)-A(0)}{s+\rho(1-s)} = L[\theta mP_{H}\beta_{H}RZ - (k+\mu_{H})A], \\ \dfrac{sL(Y)-Y(0)}{s+\rho(1-s)} = L[P_{H}\beta_{Z}(I+\sigma A)X - (\xi+\mu_{v})Y], \\ \dfrac{sL(Z)-Z(0)}{s+\rho(1-s)} = L[\xi Y - \mu_{v}Z]. \end{cases} \tag{43}$$

Now, we have

$$\begin{cases} L(I) - \dfrac{I_0}{s} - \dfrac{s+\rho(1-s)}{s} L[mP_H\beta_H SZ - (\varepsilon + \mu_H)I] = 0, \\ L(R) - \dfrac{R_0}{s} - \dfrac{s+\rho(1-s)}{s} L[\varepsilon I + kA - (\theta m P_H \beta_H Z + \tau + \mu_H)R] = 0, \\ L(A) - \dfrac{A_0}{s} - \dfrac{s+\rho(1-s)}{s} L[\theta m P_H \beta_H RZ - (k + \mu_H)A] = 0, \\ L(Y) - \dfrac{Y_0}{s} - \dfrac{s+\rho(1-s)}{s} L[P_H \beta_Z (I + \sigma A)X - (\xi + \mu_v)Y] = 0, \\ L(Z) - \dfrac{Z_0}{s} - \dfrac{s+\rho(1-s)}{s} L[\xi Y - \mu_v Z] = 0, \end{cases} \tag{44}$$

We define the nonlinear operator as follows

$$\begin{cases} N_1(\varphi_1(t;p), ..., \varphi_5(t;p)) \\ = L(\varphi_1(t;p)) - \dfrac{I_0}{s} - \dfrac{s+\rho(1-s)}{s} L[mP_H\beta_H S\varphi_5(t;p) - (\varepsilon + \mu_H)\varphi_1(t;p)], \\ N_2(\varphi_1(t;p), ..., \varphi_5(t;p)) \\ = L(\varphi_2(t;p)) - \dfrac{R_0}{s} - \dfrac{s+\rho(1-s)}{s} L[\varepsilon\varphi_1(t;p) + k\varphi_3(t;p) - (\theta m P_H\beta_H\varphi_5(t;p) + \tau + \mu_H)\varphi_2(t;p)], \\ N_3(\varphi_1(t;p), ..., \varphi_5(t;p)) \\ = L(\varphi_3(t;p)) - \dfrac{A_0}{s} - \dfrac{s+\rho(1-s)}{s} L[\theta m P_H\beta_H\varphi_2(t;p)\varphi_5(t;p) - (k + \mu_H)\varphi_3(t;p)], \\ N_4(\varphi_1(t;p), ..., \varphi_5(t;p)) \\ = L(\varphi_4(t;p)) - \dfrac{Y_0}{s} - \dfrac{s+\rho(1-s)}{s} L[P_H\beta_Z(\varphi_1(t;p) + \sigma\varphi_3(t;p))X - (\xi + \mu_v)\varphi_4(t;p)], \\ N_5(\varphi_1(t;p), ..., \varphi_5(t;p)) \\ = L(\varphi_5(t;p)) - \dfrac{Z_0}{s} - \dfrac{s+\rho(1-s)}{s} L[\xi\varphi_4(t;p) - \mu_v\varphi_5(t;p)], \end{cases} \tag{45}$$

and using Eq. (45), the zero order deformation equations can be defined as

$$\begin{cases} (1-p)L[\varphi_1(t;p)-I_0(t)] = p\hbar H(t)N_1(\varphi_1(t;p),...,\varphi_5(t;p)), \\ (1-p)L[\varphi_2(t;p)-R_0(t)] = p\hbar H(t)N_2(\varphi_1(t;p),...,\varphi_5(t;p)), \\ (1-p)L[\varphi_3(t;p)-A_0(t)] = p\hbar H(t)N_3(\varphi_1(t;p),...,\varphi_5(t;p)), \\ (1-p)L[\varphi_4(t;p)-Y_0(t)] = p\hbar H(t)N_4(\varphi_1(t;p),...,\varphi_5(t;p)), \\ (1-p)L[\varphi_5(t;p)-Z_0(t)] = p\hbar H(t)N_5(\varphi_1(t;p),...,\varphi_5(t;p)), \end{cases} \tag{46}$$

where $p \in [0,1]$ is the embedding parameter, $\hbar \neq 0$ and $H(t) \neq 0$ are the auxiliary parameter and function and L shows an auxiliary linear operator. Also, $\varphi_j(t;p)$ for j=1,2,3,4,5 are unknown functions and $I_0(t), R_0(t), A_0(t), Y_0(t)$ and $Z_0(t)$ are the initial guesses of $I(t), R(t), A(t), Y(t)$ and $Z(t)$. By replacing 0,1 instead of p we get

$$\begin{cases} \varphi_1(t;0) = I_0(t), & \varphi_1(t;1) = I(t), \\ \varphi_2(t;0) = R_0(t), & \varphi_2(t;1) = R(t), \\ \varphi_3(t;0) = A_0(t), & \varphi_3(t;1) = A(t), \\ \varphi_4(t;0) = Y_0(t), & \varphi_4(t;1) = Y(t), \\ \varphi_5(t;0) = Z_0(t), & \varphi_5(t;1) = Z(t), \end{cases} \tag{47}$$

thus clearly we can see that by increasing p from 0 to 1, the solution can be produced from initial guesses $I_0(t), R_0(t), A_0(t), Y_0(t)$ and $Z_0(t)$ to the solutions $I(t), R(t), A(t), Y(t)$ and $Z(t)$. Applying Taylor series we get

$$\begin{cases} \varphi_1(t;p) = I_0 + \sum_{m=1}^{\infty} I_m(t)p^m, \\ \varphi_2(t;p) = R_0 + \sum_{m=1}^{\infty} R_m(t)p^m, \\ \varphi_3(t;p) = A_0 + \sum_{m=1}^{\infty} A_m(t)p^m, \\ \varphi_4(t;p) = Y_0 + \sum_{m=1}^{\infty} Y_m(t)p^m, \\ \varphi_5(t;p) = Z_0 + \sum_{m=1}^{\infty} Z_m(t)p^m, \end{cases} \tag{48}$$

where $I_m(t) = \frac{1}{m!}\frac{\partial^m \varphi_1(t;p)}{\partial p^m}\Big|_{p=0}, R_m(t) = \frac{1}{m!}\frac{\partial^m \varphi_2(t;p)}{\partial p^m}\Big|_{p=0}, A_m(t) = \frac{1}{m!}\frac{\partial^m \varphi_3(t;p)}{\partial p^m}\Big|_{p=0}, Y_m(t) = \frac{1}{m!}\frac{\partial^m \varphi_4(t;p)}{\partial p^m}\Big|_{p=0}$ and $Z_m(t) = \frac{1}{m!}\frac{\partial^m \varphi_5(t;p)}{\partial p^m}\Big|_{p=0}$. By choosing suitable values for auxiliary functions and parameters, series (48) will be convergent at $p = 1$ and we have

$$\begin{cases} I(t) = I_0 + \sum_{m=1}^{\infty} I_m(t), \\ R(t) = R_0 + \sum_{m=1}^{\infty} R_m(t), \\ A(t) = A_0 + \sum_{m=1}^{\infty} A_m(t), \\ Y(t) = Y_0 + \sum_{m=1}^{\infty} Y_m(t), \\ Z(t) = Z_0 + \sum_{m=1}^{\infty} Z_m(t). \end{cases} \tag{49}$$

The m-th order deformation equation can be constructed as follows

$$\begin{cases} L[I_m(t) - \chi_m I_{m-1}(t)] = \hbar H R_{1,m}(I_{m-1}), \\ L[R_m(t) - \chi_m R_{m-1}(t)] = \hbar H R_{2,m}(R_{m-1}), \\ L[A_m(t) - \chi_m A_{m-1}(t)] = \hbar H R_{3,m}(A_{m-1}), \\ L[Y_m(t) - \chi_m Y_{m-1}(t)] = \hbar H R_{4,m}(Y_{m-1}), \\ L[Z_m(t) - \chi_m Z_{m-1}(t)] = \hbar H R_{5,m}(Z_{m-1}), \end{cases} \tag{50}$$

where

$$\begin{cases} R_{1,m}(\vec{I}_{m-1}(t), \vec{R}_{m-1}(t), \vec{A}_{m-1}(t), \vec{Y}_{m-1}(t), \vec{Z}_{m-1}(t)) \\ = L(I_{m-1}) - \dfrac{I_0}{s}(1-\chi_m) - \dfrac{s+\rho(1-s)}{s} L[mP_H\beta_H S_{m-1}Z_{m-1} - (\varepsilon+\mu_H)I_{m-1}], \\ R_{2,m}(\vec{I}_{m-1}(t), \vec{R}_{m-1}(t), \vec{A}_{m-1}(t), \vec{Y}_{m-1}(t), \vec{Z}_{m-1}(t)) \\ = L(R_{m-1}) - \dfrac{R_0}{s}(1-\chi_m) - \dfrac{s+\rho(1-s)}{s} L[\varepsilon I_{m-1} + kA_{m-1} - (\theta mP_H\beta_H Z_{m-1} + \tau + \mu_H)R_{m-1}], \\ R_{3,m}(\vec{I}_{m-1}(t), \vec{R}_{m-1}(t), \vec{A}_{m-1}(t), \vec{Y}_{m-1}(t), \vec{Z}_{m-1}(t)) \\ = L(A_{m-1}) - \dfrac{A_0}{s}(1-\chi_m) - \dfrac{s+\rho(1-s)}{s} L[\theta mP_H\beta_H R_{m-1}Z_{m-1} - (k+\mu_H)A_{m-1}], \\ R_{4,m}(\vec{I}_{m-1}(t), \vec{R}_{m-1}(t), \vec{A}_{m-1}(t), \vec{Y}_{m-1}(t), \vec{Z}_{m-1}(t)) \\ = L(Y_{m-1}) - \dfrac{Y_0}{s}(1-\chi_m) - \dfrac{s+\rho(1-s)}{s} L[P_H\beta_Z(I_{m-1} + \sigma A_{m-1})X_{m-1} - (\xi+\mu_v)Y_{m-1}], \\ R_{5,m}(\vec{I}_{m-1}(t), \vec{R}_{m-1}(t), \vec{A}_{m-1}(t), \vec{Y}_{m-1}(t), \vec{Z}_{m-1}(t)) \\ = L(Z_{m-1}) - \dfrac{Z_0}{s}(1-\chi_m) - \dfrac{s+\rho(1-s)}{s} L[\xi Y_{m-1} - \mu_v Z_{m-1}]. \end{cases} \tag{51}$$

Applying inverse Laplace transform for both sides of the m-th order deformation equation (50) we get

$$\begin{cases} I_m(t) = \chi_m I_{m-1}(t) + \hbar H L^{-1}[R_{1,m}(I_{m-1})], \\ R_m(t) = \chi_m R_{m-1}(t) + \hbar H L^{-1}[R_{2,m}(R_{m-1})], \\ A_m(t) = \chi_m A_{m-1}(t) + \hbar H L^{-1}[R_{3,m}(A_{m-1})], \\ Y_m(t) = \chi_m Y_{m-1}(t) + \hbar H L^{-1}[R_{4,m}(Y_{m-1})], \\ Z_m(t) = \chi_m Z_{m-1}(t) + \hbar H L^{-1}[R_{5,m}(Z_{m-1})], \end{cases} \tag{52}$$

and it can help us to find the iterations of the HATM.

7 CESTAC method-CADNA library

As we know, usual numerical and semi analytical methods for solving mathematical and engineering problems are based on the FPA. But because of the mentioned problems, it will be better if we replace the FPA by a random arithmetic. For this aim, we apply the DSA which has many applications and advantages than other arithmetics. Thus, we apply the CESTAC method and the CADNA library to validate the numerical results. For more information about this method please see [1, 11].

By collecting all representable values which are produced by computer in set B, we can write $S^* \in B$ for $s^* \in \mathbb{R}$ with α mantissa bits of the binary FPA as

$$S^* = s^* - \rho 2^{E-\alpha}\phi, \tag{53}$$

where sign, missing segment of the mantissa and the binary exponent of the result are demonstrated by $\rho, 2^{-\alpha}\phi$ and E respectively [8, 9, 16, 17]. In order to find the results with single and double precisions, the value α can be changed to 24 and 53. Let ϕ be a casual variable that uniformly distributed on $[-1, 1]$, constructing perturbation on last mantissa bit of s^*, the mean (μ) and the standard deviation (σ) values can be produced for results of S^*. Doing the process for k times, we will have the quasi Gaussian distribution on $S_i^*, i = 1, \cdots, k$ and we will have equality between μ and the exact s^*. The following algorithm is presented to show the process step by step, where τ_δ is the value of T distribution as the confidence interval is $1-\delta$, with $k-1$ freedom degree [18, 50, 51].

Algorithm 1:

`Step 1- Make` k `samples of` S^* `as` $\Phi = \{S_1^*, S_2^*, ..., S_k^*\}$ `by constructing perturbation on the last bit of mantissa.`

`Step 2- Find` $\tilde{S}^* = \dfrac{\sum_{i=1}^{k} S_i^*}{k}$.

`Step 3- Compute` $\sigma^2 = \dfrac{\sum_{i=1}^{k}(S_i^* - \tilde{S}^*)^2}{k-1}$.

`Step 4- Find the number of common significant digits between` S^* `and` $\tilde{S}^*$`, using` $C_{\tilde{S}^*,S^*} = \log_{10} \dfrac{\sqrt{k}\left|\tilde{S}^*\right|}{\tau_\delta \sigma}$.

`Step 5- Show` $S^* = @.0$ `if` $\tilde{S}^* = 0$`, or` $C_{\tilde{S}^*,S^*} \leq 0$.

When we want to apply the CESTAC method, instead of using the algorithm directly, we should apply the CADNA library. The library can implement the algorithm automatically. The CADNA library should be done on Linux operating system and all codes should be improved by C, C++, FORTRAN or ADA codes. So in this method we do not need to apply the usual mathematical softwares such as Mathematica, Maple and MATLAB. Applying the CESTAC method and DSA we have some advantages in comparison with the methods based on the FPA. In order to apply the termination criterion (1) which is based on the FPA we need to have the exact solution but in the DSA we do not need to the exact solution and stopping condition (2) is based on two successive approximations [11]. In the FPA, we do not know the optimal

ε and in the DSA we do not have value ε definitely. In the FPA, the extra iterations can be produced without improving the accuracy, but in the DSA we can find the optimal number of iterations. In the FPA, the algorithm can be stopped in the first step without producing the accurate results but in the DSA, the optimal approximation can be identified. In the CESTAC method, we can produce @.0 which shows the number of common significant digits between two successive approximations is zero but in the FPA we can not produce this sign. In next, we have the sample code of the CADNA library:

```
# include <cadna.h>
cadna_init(-1);
main()
{
double_st Parameter;
do
{
Write the main program here;
printf(" %s ",strp(Parameter));
}
while(u[n]-u[n-1]!=0);
cadna_end();
}
```

Definition 7.1. *[11] For two real numbers ω_1 and ω_2, the number of common significant digits can be defined as*

$$\begin{cases} C_{\omega_1,\omega_2} = \log_{10}\left|\dfrac{\omega_1+\omega_2}{2(\omega_1-\omega_2)}\right| = \log_{10}\left|\dfrac{\omega_1}{\omega_1-\omega_2}-\dfrac{1}{2}\right|, & \omega_1 \neq \omega_2, \\ C_{\omega_1,\omega_1} = +\infty. \end{cases} \tag{54}$$

Theorem 7.1. *Let*

$$I_m(t) = \textstyle\sum_{j=0}^m I_j(t), \quad R_m(t) = \sum_{j=0}^m R_j(t), \quad A_m(t) = \sum_{j=0}^m A_j(t),$$

$$Y_m(t) = \textstyle\sum_{j=0}^m Y_j(t), \quad Z_m(t) = \sum_{j=0}^m Z_j(t),$$

be the approximate solution of the mathematical model of Malaria infection (9) which is produced by the HATM and based on the convergence control parameter $\hbar$ independent of m, then

$$\begin{aligned} C_{I_m,I_{m+1}} &= C_{I_m,I} + O(\tfrac{1}{m}), \\ C_{R_m,R_{m+1}} &= C_{R_m,R} + O(\tfrac{1}{m}), \\ C_{A_m,A_{m+1}} &= C_{A_m,A} + O(\tfrac{1}{m}), \\ C_{Y_m,Y_{m+1}} &= C_{Y_m,Y} + O(\tfrac{1}{m}), \\ C_{Z_m,Z_{m+1}} &= C_{Z_m,Z} + O(\tfrac{1}{m}), \end{aligned} \tag{55}$$

Proof: Using Definition 7.1 we have

$$\begin{aligned} C_{I_m,I_{m+1}} - C_{I_m,I} &= \log_{10}\left|\frac{I_m+I_{m+1}}{2(I_m-I_{m+1})}\right| - \log_{10}\left|\frac{I_m+I}{2(I_m-I)}\right| \\ &= \log_{10}\left|\frac{I_m+I_{m+1}}{2(I^{\hbar}_{m+1})}\right| - \log_{10}\left|\frac{I_m+I}{2(I_m-I)}\right| \\ &= \log_{10}\left|\frac{I_m+I_{m+1}}{I_m+I}\right| + \log_{10}\left|\frac{I_m-I}{I^{\hbar}_{m+1}}\right|. \end{aligned} \tag{56}$$

By increasing the iterations number m, we can see in the first term of Eq. (56), the approximate and exact solutions I_m, I are close together and we can neglect that. For the second term we have

$$\begin{aligned} \log_{10}\left|\frac{I_m-I}{I_{m+1}}\right| &= \log_{10}\left|\frac{\sum_{i=0}^{m} I_i - \sum_{i=0}^{\infty} I_i}{I_{m+1}}\right| \\ &= \log_{10}\left|\frac{\sum_{i=m+1}^{\infty} I_i}{I_{m+1}}\right| \\ &= \log_{10}\left|1+\frac{\sum_{i=m+2}^{\infty}\hbar L^{-1}\big[H(r)\Re_i(u_{i-1})\big]}{\hbar L^{-1}\big[H(r)\Re_{m+1}(u_m)\big]}\right|. \end{aligned}$$

Based on Eqs. (6) and (7) we can write

$$\begin{aligned} &\frac{\sum_{i=m+2}^{\infty}\hbar L^{-1}\big[H(r)\Re_i(u_{i-1})\big]}{\hbar L^{-1}\big[H(r)\Re_{m+1}(u_m)\big]} = \frac{\sum_{i=m+2}^{\infty}\hbar L^{-1}\left[H(r)\frac{1}{(i-1)!}\frac{\partial^{i-1}N[U(r,v)]}{\partial v^{i-1}}\bigg|_{v=0}\right]}{\hbar L^{-1}\left[H(r)\frac{1}{m!}\frac{\partial^{m}N[U(r,v)]}{\partial v^{m}}\bigg|_{v=0}\right]} \\ &= \frac{\hbar L^{-1}\left[H(r)\frac{1}{(m+1)!}\frac{\partial^{m+1}N[U(r,v)]}{\partial v^{m+1}}\bigg|_{v=0}\right]}{\hbar L^{-1}\left[H(r)\frac{1}{m!}\frac{\partial^{m}N[U(r,v)]}{\partial v^{m}}\bigg|_{v=0}\right]} + \frac{\hbar L^{-1}\left[H(r)\frac{1}{(m+2)!}\frac{\partial^{m+2}N[U(r,v)]}{\partial v^{m+2}}\bigg|_{v=0}\right]}{\hbar L^{-1}\left[H(r)\frac{1}{m!}\frac{\partial^{m}N[U(r,v)]}{\partial v^{m}}\bigg|_{v=0}\right]} + \cdots \\ &= O(\frac{1}{m}). \end{aligned}$$

Therefore, we get

$$\log_{10}\left|\frac{I_m-I}{I_{m+1}}\right| = \log_{10}\left|1+O(\frac{1}{m})\right|.$$

By repeating the process for other terms we have

$$\log_{10}\left|\frac{R_m - R}{R_{m+1}}\right| = \log_{10}\left|1 + O(\frac{1}{m})\right|,$$

$$\log_{10}\left|\frac{A_m - A}{A_{m+1}}\right| = \log_{10}\left|1 + O(\frac{1}{m})\right|,$$

$$\log_{10}\left|\frac{Y_m - Y}{Y_{m+1}}\right| = \log_{10}\left|1 + O(\frac{1}{m})\right|,$$

$$\log_{10}\left|\frac{Z_m - Z}{Z_{m+1}}\right| = \log_{10}\left|1 + O(\frac{1}{m})\right|.$$

Since $O(\frac{1}{m}) << 1$, then the right hand side of above relation decreases as m increases. Thus, the proof is complete.$\square$

Theorem 7.1 is proved for fixed value of convergence control parameter $\hbar$. This theorem allows us to apply the new termination criterion which is based on two successive approximations instead of absolute error and it shows the equality between the number of common significant digits of difference between two successive approximations and difference between exact and approximate solutions which in the CESTAC method it can be shown by @.0.

8 Numerical Results

In this section, the numerical results of validation of the HATM based on both the SA and the FPA are presented. We know that HATM is one of flexible methods which this is because of existence of auxiliary parameters and functions. They are help us to make accurate solutions with fast convergence rate. Parameter $\hbar$ is to control the convergence region of the HATM. We know that the obtained solution using the HATM are based on t and $\hbar$. Thus we will be able to plot the $\hbar$-curve to find the convergence region. These area is the parallel part of the $\hbar$-curve with axiom x. In Figs. (1) and (2) the convergence region for $m = 5, 10$ are demonstrated. Based on these figures these region for $m = 5$, $\rho = 1$ and $t = 1$ are

$$\begin{gathered} -1.2 \preceq \hbar_{I,5} \preceq -0.7, \\ -1.2 \preceq \hbar_{R,5} \preceq -0.7, \\ -1.3 \preceq \hbar_{A,5} \preceq -0.6, \\ -1.1 \preceq \hbar_{Y,5} \preceq -0.7, \\ -1.1 \preceq \hbar_{Z,5} \preceq -0.8, \end{gathered}$$

and for $m = 10$ are

$$\begin{gathered} -1.5 \preceq \hbar_{I,10} \preceq -0.5, \\ -1.5 \preceq \hbar_{R,10} \preceq -0.5, \\ -1.4 \preceq \hbar_{A,10} \preceq -0.5, \\ -1.2 \preceq \hbar_{Y,10} \preceq -0.7, \\ -1.2 \preceq \hbar_{Z,10} \preceq -0.7. \end{gathered}$$

Table 2: The residual error based on the FPA for $\rho = 1$, $\hbar = -1$ and $m = 5, 10$.

m	t	$I(t)$	$R(t)$	$A(t)$	$Y(t)$	$Z(t)$
5	0.0	4.44089×10^{-16}	6.93889×10^{-18}	3.46945×10^{-17}	0	0
	0.2	8.12273×10^{-10}	1.89021×10^{-10}	2.13396×10^{-10}	2.46061×10^{-9}	3.39051×10^{-8}
	0.4	2.64273×10^{-8}	6.10971×10^{-9}	6.8897×10^{-9}	9.58309×10^{-8}	1.08496×10^{-6}
	0.6	2.03836×10^{-7}	4.68418×10^{-8}	5.27648×10^{-8}	8.546×10^{-7}	8.23893×10^{-6}
	0.8	8.71662×10^{-7}	1.99201×10^{-7}	2.2416×10^{-7}	4.12401×10^{-6}	0.0000347188
	1.0	2.69711×10^{-6}	6.13229×10^{-7}	6.89399×10^{-7}	0.0000141451	0.000105953
10	0.0	1.26565×10^{-14}	9.02056×10^{-17}	9.36751×10^{-16}	4.61853×10^{-14}	0
	0.2	1.28786×10^{-14}	1.17961×10^{-16}	1.02002×10^{-15}	6.75016×10^{-14}	4.17444×10^{-14}
	0.4	1.22125×10^{-14}	1.66533×10^{-16}	1.10328×10^{-15}	2.77112×10^{-13}	1.33227×10^{-13}
	0.6	3.05589×10^{-14}	3.45557×10^{-15}	1.29757×10^{-15}	9.66338×10^{-13}	2.20268×10^{-13}
	0.8	3.29958×10^{-13}	4.66849×10^{-14}	5.17086×10^{-14}	1.30456×10^{-11}	1.49925×10^{-12}
	1.0	3.00837×10^{-12}	4.40259×10^{-13}	4.89914×10^{-13}	1.13957×10^{-10}	1.5433×10^{-11}

In Fig. (3), the residual error functions based on $\hbar$ for $t = 1$ and $m = 5, 10$ are plotted. Using this graph, obviously we can see the regions of convergence for different functions where for $m = 5$ and $-1.2 \preceq \hbar \preceq -0.7$ we will have accurate results that other regions. Also, for $m = 5$ we have $-1.3 \preceq \hbar \preceq -0.5$. Fig. (4), shows the residual error functions based on t for $\hbar = -1$ and $m = 5, 10$. Completely clear that by increasing number of iterations m from 5 to 10 the HATM can produce more accurate results. In Table 2, the numerical results of $I(t), R(t), A(t), Y(t)$ and $Z(t)$ are presented based on the FPA for $m = 5, 10$ and $\hbar = -1$. But in these results which are based on the FPA, the optimal number of iterations and the optimal approximations can not be identified. Also, we do not know that what is the termination criterion to stop the algorithm at steps $m = 5$ and $m = 10$. Because of the mentioned problems, we use the CESTAC method and the CADNA library which are based on the SA. Table 3, shows the results applying the CESTAC method. Thus instead of applying the absolute error or residual error, by finding difference of two successive approximations we can show the accuracy of the results and the main theorem 7.1 supports us to do it. Using this technique, not only we do not need to have the exact solution but also we can find the optimal iteration and the optimal approximations. Thus, the optimal iteration is $m_{opt} = 9$ and the optimal approximations are

$$\begin{aligned}
I_{opt}(t) &= 0.481763160360134E + 001, \\
R_{opt}(t) &= 0.149853816238038E + 002, \\
A_{opt}(t) &= 0.100188240700409E + 002, \\
Y_{opt}(t) &= 0.869982508153463E + 002 \\
Z_{opt}(t) &= 0.568682257413900E + 002.
\end{aligned}$$

sign @.0 in the ninth step shows that the number of common significant digits for two successive approximations is almost equal to the number of common significant digits for exact and approximate solutions. But this sign can be produced in the FPA and in the mathematical methods based on the FPA we need to provide a small positive value ε. Since we do not know the optimal value of ε so it can make problem in computations.

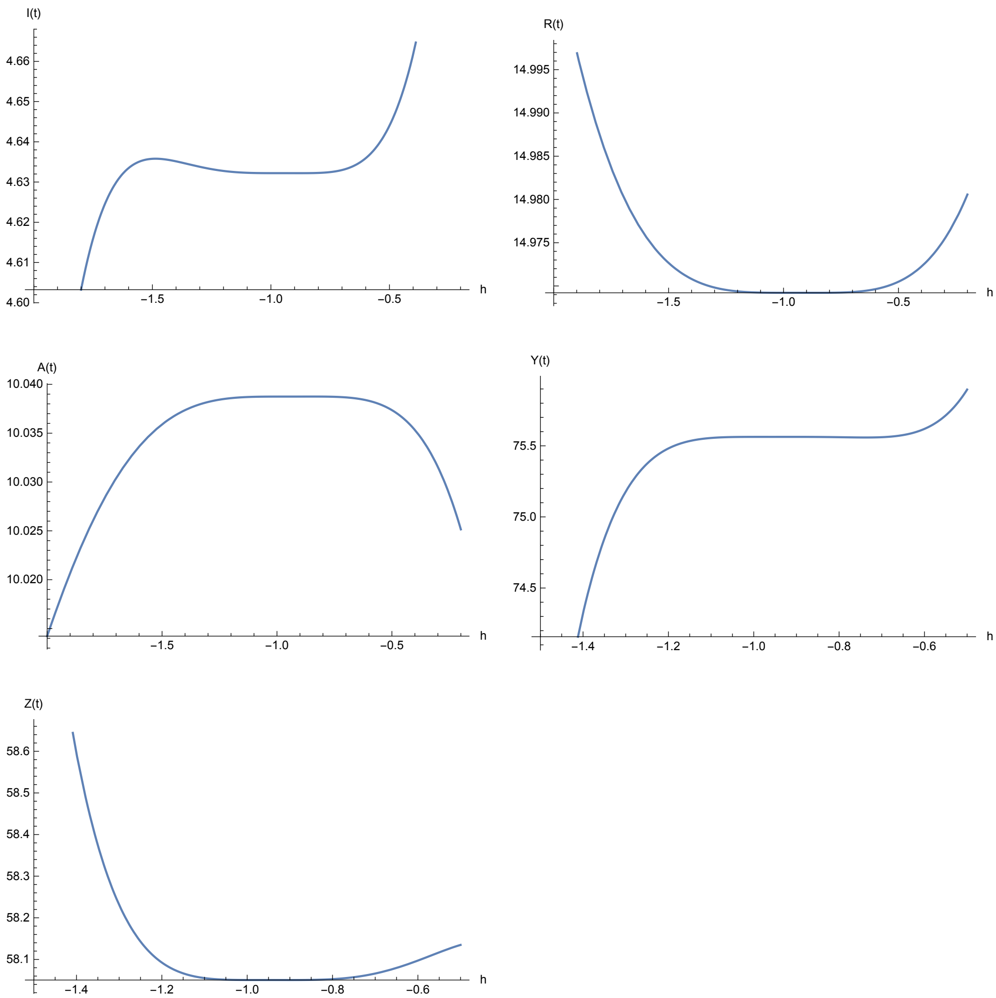

Figure 1: The $\hbar$-curves for $t = 1$ and $m = 5$.

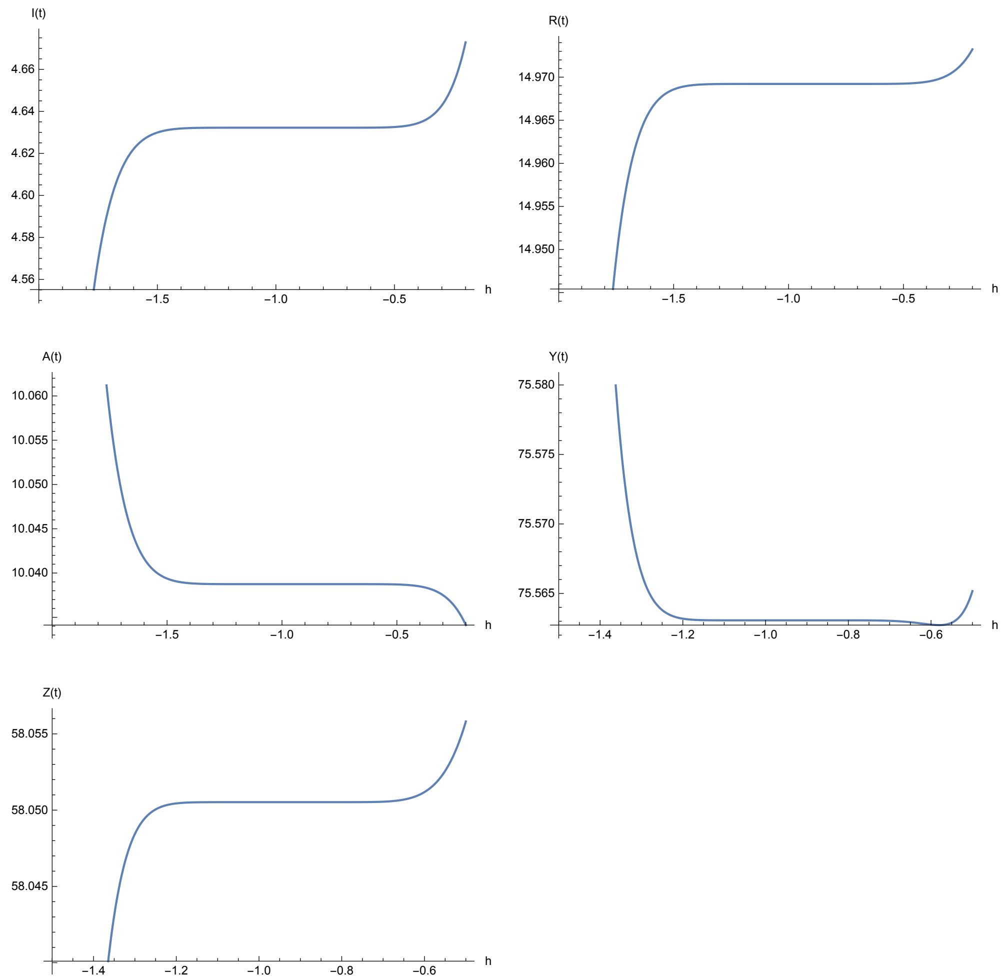

Figure 2: The $\hbar$-curves for $t = 1$ and $m = 10$.

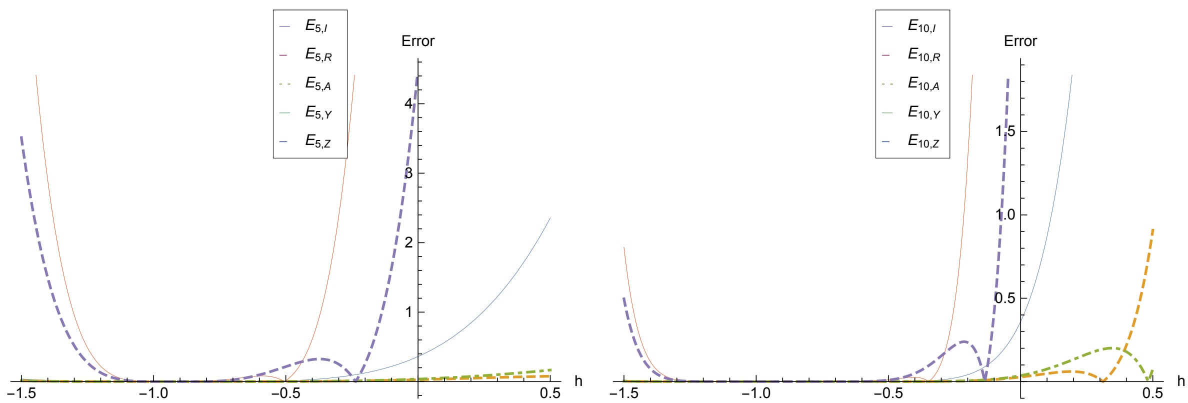

Figure 3: Graph of residual error functions based on $\hbar$ for $t = 1$ and $m = 5, 10$.

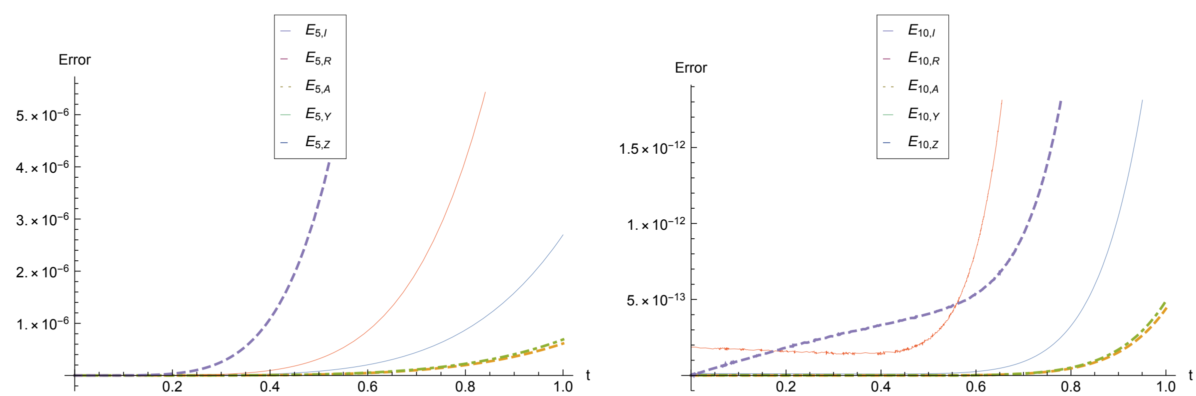

Figure 4: Graph of residual error functions based on t for $\hbar = -1$ and $m = 5, 10$.

Table 3: The numerical results using the CESTAC method for $t = 0.5, \rho = 1$ and $\hbar = -1$.

m	Approximate solutions	Difference between two iterations
1	0.481991099999999E+001	0.481991099999999E+001
	0.149863450500000E+002	0.149863450500000E+002
	0.100180841999999E+002	0.100180841999999E+002
	0.861499999999999E+002	0.861499999999999E+002
	0.572499999999999E+002	0.572499999999999E+002
2	0.481721974999999E+001	0.269125000000E-002
	0.149852798900000E+002	0.10651599999E-002
	0.100189276124999E+002	0.843412499998E-003
	0.870325624999999E+002	0.8825625000000E+000
	0.568474999999999E+002	0.40250000000000E+000
3	0.481764999124999E+001	0.43024124999E-003
	0.149853857548750E+002	0.1058648749E-003
	0.100188196841249E+002	0.1079283750E-003
	0.869973047500000E+002	0.352577499999E-001
	0.568689177500000E+002	0.214177500000E-001
4	0.481763111356249E+001	0.1887768749E-004
	0.149853816087687E+002	0.414610625E-005
	0.100188240859124E+002	0.440178750E-005
	0.869982671999999E+002	0.9624499999E-003
	0.568682093062500E+002	0.7084437500E-003
5	0.481763161019062E+001	0.49662812E-006
	0.149853816249481E+002	0.161793E-007
	0.100188240683186E+002	0.175938E-007
	0.869982507985312E+002	0.16401468E-004
	0.568682260151874E+002	0.167089374E-004
6	0.481763160369595E+001	0.649467E-008
	0.149853816238078E+002	0.11402E-008
	0.100188240700391E+002	0.17204E-008
	0.869982508141096E+002	0.15578E-007
	0.568682257392671E+002	0.2759203E-006
7	0.481763160360170E+001	0.9425E-010
	0.149853816238027E+002	0.513E-011
	0.100188240700421E+002	0.292E-011
	0.869982508158002E+002	0.16906E-008
	0.568682257413493E+002	0.20821E-008
8	0.481763160360176E+001	0.6E-013
	0.149853816238039E+002	0.122E-011
	0.100188240700408E+002	0.12E-011
	0.869982508153463E+002	0.4539E-009
	0.568682257413900E+002	0.407E-010
9	0.481763160360134E+001	0.41E-012
	0.149853816238038E+002	0.4E-013
	0.100188240700409E+002	0.4E-013
	0.869982508153463E+002	@.0
	0.568682257413900E+002	@.0

9 Conclusion

Mathematical models have special roles to predict various phenomena. In this paper, the non-linear fractional model of Malaria infection was investigated. Using the fractional models we can produce more accurate results than other usual models. For this aim we applied the Caputo-Fabrizio fractional derivative. Also, the Picard-Lindelof approach and the Banach fixed point theorem were used to show the existence of solution and the stability of the method. The HATM was applied to solve the mentioned model and the DSA was used to validate the results. Using the CESTAC method and the CADNA library which are based on the DSA, we can find the optimal iteration and the optimal approximation of the model. So we do not need to apply the traditional absolute error or residual error to show the accuracy. Instead of them we apply new termination criterion which is based on two successive approximations. The main theorem of the CESTAC method was proved which it can support us to use the new termination criterion. In the numerical results by plotting several $\hbar$-curves we showed the convergence regions. Also, the numerical results based on the FPA and DSA were presented in some tables. According to the obtained results, we can see the advantages of the DSA than FPA. In the DSA, we do not need to make more and extra iterations. Also, we can find the optimal iteration and optimal approximations. But in the FPA, we do not have these abilities. More over in the DSA, the informatical zero sign @.0 can be produced which shows that the number of common significant digits for to successive approximations is almost equal to the number of common significant digits for exact and approximate solutions and the numerical algorithm can be stopped. But in the FPA, the stopping condition depends on a small positive value ε that we do not have information about its optimality. Applying the method on the fractional models of HIV infection and COVID-19 are among our future plans.

Acknowledgments: A. Dreglea and S. Noeiaghdam are supported by a grant from the Academic Council in the direction of the scientific school of Irkutsk National Research Technical University No. 14-NSH-RAN-2020.

References

[1] `https://www-pequan.lip6.fr/`

[2] `https://www.who.int/health-topics/malaria#tab=tab_1`

[3] T. Abdeljawad, D. Baleanu, On fractional derivatives with exponential kernel and their discrete versions, Rep. Math. Phys. 80(1) (2017) 11–27.

[4] S.M. Aydogan, D. Baleanu, A. Mousalou, S. Rezapour, On high order fractional integro-differential equations including the Caputo–Fabrizio derivative, Bound. Value Probl. 2018, 90 (2018).

[5] F.B.M. Belgacem, A.A. Karaballi, S.L. Kalla, Analytical investigations of the Sumudu transform and applications to integral production equations, Math. Probl. Eng. 3 (2003) 103–118.

[6] D.S. Bodkhe, S.K. Panchal, On Sumudu transform of fractional derivatives and its applications to fractional differential equations, Asian J. Math. Comput. Res. 11(1) (2016) 69–77.

[7] M. Caputo, M. Fabrizio, A new definition of fractional derivative without singular kernel, Prog. Fract. Differ. Appl. 1(2) (2015) 73–85.

[8] J.M. Chesneaux, CADNA, an ADA tool for round–off error analysis and for numerical debugging, In Proceedings of the Congress on ADA, Aerospace, Barcelona, 20–25 May 1990.

[9] J.M. Chesneaux, F. Jézéquel, Dynamical control of computations using the Trapezoidal and Simpson's rules, J. Univers. Comput. Sci. 4 (1998) 2–10.

[10] M. A. Fariborzi Araghi, S. Noeiaghdam, A novel technique based on the homotopy analysis method to solve the first kind Cauchy integral equations arising in the theory of airfoils, Journal of Interpolation and Approximation in Scientific Computing, 2016 (1) (2016) 1-13.

[11] M. A. Fariborzi Araghi, S. Noeiaghdam, Validation of Numerical Algorithms: Stochastic Arithmetic, Entekhab Bartar Publisher, Iran, 2021. ISBN: 978-622-6498-09-8.

[12] M. A. Fariborzi Araghi, S. Noeiaghdam, Finding the optimal step of fuzzy Newton-Cotes integration rules by using CESTAC method, Journal of Fuzzy Set Valued Analysis, 2 (2017) 62-85.

[13] M. A. Fariborzi Araghi, S. Noeiaghdam, A valid scheme to evaluate fuzzy definite integrals by applying the CADNA library, International Journal of Fuzzy System Applications, 6 (4) (2017) 1-20.

[14] M. A. Fariborzi Araghi, S. Noeiaghdam, Dynamical control of computations using the Gauss-Laguerre integration rule by applying the CADNA library, Advances and Applications in Mathematical Sciences, 16 (2016) 1-18.

[15] L. L.Fonseca, E. O.Voit, Comparison of mathematical frameworks for modeling erythropoiesis in the context of malaria infection, Mathematical Biosciences, 270 (2015) 224-236.

[16] S. Graillat, F. Jézéquel, S. Wang, Y. Zhu, Stochastic arithmetic in multi precision, Math. Comput. Sci. 5 (2011) 359–375.

[17] S. Graillat, F. Jézéquel, R. Picot, Numerical Validation of Compensated Summation Algorithms with Stochastic Arithmetic, Electron. Notes Theor. Comput. Sci. 317 (2015) 55–69.

[18] F. Jézéquel, C.R. Mecanique, A dynamical strategy for approximation methods, Comptes Rendus Mec. 334 (2006) 362–367.

[19] E. Khoshrouye Ghiasi, S. Noeiaghdam, Truncating the series expansion for unsteady velocity-dependent Eyring-Powell fluid, Eng. Appl. Sci. Lett., 3(4) (2020) 28-34; https://doi.org/10.30538/psrp-easl2020.0049

[20] J. E. Kim, Y. Choi, C. H. Lee, Effects of climate change on Plasmodium vivax malaria transmission dynamics: A mathematical modeling approach, Applied Mathematics and Computation, 347 (15) (2019) 616-630.

[21] S. J. Liao, Beyond Perturbation: Introduction to Homotopy Analysis Method, Chapman & Hall/CRC Press, Boca Raton, (2003).

[22] S. J. Liao, Homotopy analysis method in nonlinear differential equations, Higher Education Press, Beijing and Springer-Verlag Berlin Heidelberg, (2012).

[23] S. J. Liao, The proposed homotopy analysis techniques for the solution of nonlinear problems, Ph.D. Thesis, Shanghai Jiao Tong University, Shanghai, (1992).

[24] J. Losada, J.J. Nieto, Properties of the new fractional derivative without singular kernel, Prog. Fract. Differ. Appl. 1(2), 87–92 (2015).

[25] R.C. Mittal, Rohit Goel, Neha Ahlawat, An Efficient Numerical Simulation of a Reaction-Diffusion Malaria Infection Model using B-splines Collocation, Chaos, Solitons & Fractals, 143 (2021) 110566.

[26] P. A. Naik, J. Zu, K. M. Owolabi, Modeling the mechanics of viral kinetics under immune control during primary infection of HIV-1 with treatment in fractional order, Physica A: Statistical Mechanics and its Applications 545, 123816 (2020).

[27] P. A. Naik, M. Yavuz, J. Zu, The role of prostitution on HIV transmission with memory: A modeling approach, Alexandria Eng J 59(4) (2020) 2513-2531.

[28] P. A. Naik, J. Zu, K. M. Owolabi, Global dynamics of a fractional order model for the transmission of HIV epidemic with optimal control, Chaos Solitons Fractals 138, 109826 (2020).

[29] S. Noeiaghdam, Numerical Approximation of Modified Non-linear SIR Model of Computer Viruses, Contemporary Mathematics, 1 (1), (2019).

[30] S. Noeiaghdam, A novel technique to solve the modified epidemiological model of computer viruses. SeMA Journal, 76, 97–108 (2019).

[31] S. Noeiaghdam, M. A. Fariborzi Araghi, Homotopy regularization method to solve the singular Volterra integral equations of the first kind, Jordan Journal of Mathematics and Statistics (JJMS), 11 (1), (2018), 1-12.

[32] S. Noeiaghdam, M. A. Fariborzi Araghi, A novel approach to find optimal parameter in the homotopy-regularization method for solving integral equations, Applied Mathematics and Information Sciences, 14 (1), 1-8 (2020).

[33] S. Noeiaghdam, M. A. Fariborzi Araghi, S. Abbasbandy, Finding optimal convergence control parameter in the homotopy analysis method to solve integral equations based on the stochastic arithmetic, Numerical Algorithms, 81 (1), 237-267 (2019).

[34] S. Noeiaghdam, M. A. Fariborzi Araghi, A novel algorithm to evaluate definite integrals by the Gauss-Legendre integration rule based on the stochastic arithmetic: Application in the model of osmosis system, Mathematical Modelling of Engineering Problems, 7 (4) (2020), 577-586. https://doi.org/10.18280/mmep.070410

[35] S. Noeiaghdam, M.A. Fariborzi Araghi, S. Abbasbandy, Valid implementation of Sinc-collocation method to solve the fuzzy Fredholm integral equation, Journal of Computational and Applied Mathematics, 370 (2020) 112632.

[36] S. Noeiaghdam, M. A. Fariborzi Araghi, Valid implementation of the Sinc-collocation method to solve the linear integral equations by CADNA library. Journal of Mathematical Modeling, (2019).

[37] S. Noeiaghdam, A. Dreglea, J. H. He, Z. Avazzadeh, M. Suleman, M. A. Fariborzi Araghi, D. Sidorov, N. Sidorov, Error estimation of the homotopy perturbation method to solve second kind Volterra integral equations with piecewise smooth kernels: Application of the CADNA library, Symmetry, 12, 1730, (2020). doi.org/10.3390/sym12101730

[38] S. Noeiaghdam, K. Kamal Ali, Semi-analytical Method to Solve the Non-linear System of Equations to Model of Evolution for Smoking Habit in Spain, Int. J. Industrial Mathematics, 12 (4) (2020) Article ID IJIM-1377. Available online at http://ijim.srbiau.ac.ir/

[39] S. Noeiaghdam, E. Khoshrouye Ghiasi, An efficient method to solve the mathematical model of HIV infection for CD8+T cells, International Journal of Mathematical Modelling & Computations, 9, 4 (Fall)-Serial Number 36, (2019), 267-281.

[40] S. Noeiaghdam, D. Sidorov, Caputo-Fabrizio Fractional Derivative to Solve the Fractional Model of Energy Supply-Demand System, Mathematical Modelling of Engineering Problems, 7(3) (2020) 359-367. https://doi.org/10.18280/mmep.070305

[41] S. Noeiaghdam, D. Sidorov, A. M. Wazwaz, N. Sidorov, V. Sizikov, The numerical validation of the Adomian decomposition method for solving Volterra integral equation with discontinuous kernel using the CESTAC method, Mathematics 2021, 9, 260. https://doi.org/10.3390/math9030260

[42] S. Noeiaghdam, D. Sidorov, A. Zamyshlyaeva, A. Tynda, A. Dreglea, A valid dynamical control on the reverse osmosis system using the CESTAC method, Mathematics 2021, 9, 48. https://dx.doi.org/10.3390/math9010048

[43] S. Noeiaghdam, D. Sidorov, V. Sizikov, N. Sidorov, Control of accuracy on Taylor-collocation method to solve the weakly regular Volterra integral equations of the first kind by using the CESTAC method, Applied and Computational Mathematics an International Journal, 19 (1) (2020) 81-105.

[44] S. Noeiaghdam, D. Sidorov, I. Muftahov, A.V. Zhukov, Control of Accuracy on Taylor-Collocation Method for Load Leveling Problem, The Bulletin of Irkutsk State University. Series Mathematics, 30 (2019) 59-72.

[45] S. Noeiaghdam, M. Suleman, H. Budak, Solving a modified non-linear epidemiological model of computer viruses by homotopy analysis method. Mathematical Sciences, (2018).

[46] S. Noeiaghdam, E. Zarei, H. Barzegar Kelishami, Homotopy analysis transform method for solving Abel's integral equations of the first kind, Ain Shams Engineering Journal, 7 (2016) 483–495.

[47] K. Shah, N.A.M. Junaid, Extraction of Laplace, Sumudu, Fourier and Mellin transform from the natural transform, J. Appl. Environ. Biol. Sci. 5(9) (2015) 1–10.

[48] M. Suleman, D. Lu, J. H. He, U. Farooq, S. Noeiaghdam, F.A. Chandio, Elzaki Projected Differential Transform method for Fractional order System of Linear and Nonlinear Fractional Partial Differential Equation, Fractals, 26 (3), 1850041, (2018).

[49] N. H. Sweilam, S. M. AL–Mekhlafi, A. O. Albalawi, Optimal control for a fractional order malaria transmission dynamics mathematical model, Alexandria Engineering Journal, 59 (3) (2020) 1677-1692.

[50] J. Vignes, Discrete Stochastic Arithmetic for Validating Results of Numerical Software, Spec. Issue Numer. Algorithms 7 (2004) 377–390.

[51] J. Vignes, A stochastic arithmetic for reliable scientific computation, Math. Comput. Simul. 35 (1993) 233–261.

[52] G.K. Watugala, Sumudu transform: a new integral transform to solve differential equations and control engineering problems, Int. J. Math. Educ. Sci. Technol. 24(1) (1993) 35–43.

[53] J. Wang, Y. Zhou, M. Medved, Picard and weakly Picard operators technique for nonlinear differential equations in Banach spaces, J. Math. Anal. Appl. 389(1) (2012) 261–274.

[54] L. Yakob, Endectocide-treated cattle for malaria control: A coupled entomological-epidemiological model, Parasite Epidemiology and Control 1 (2016) 2-9.